DER MATERIALS QUARTERLY PROGRESS REPORT

For the Period
October 1, 2002 to December 31, 2002

Prepared by:

David P. Stinton, Manager, and
Roxanne A. Raschke
DER Materials Research
Oak Ridge National Laboratory

For:

Department of Energy
Office of Power Technologies
Energy Efficiency and Renewable Energy

DER MATERIALS QUARTERLY PROGRESS REPORT

October—December 2002

TABLE OF CONTENTS

MATERIALS FOR ADVANCED RECIPROCATING ENGINES

RECUPERATORS

Advanced Alloys for High-Temperature Recuperators

P. J. Maziasz, B. A. Pint, R. W. Swindeman, and K. L. More
Metals and Ceramics Division
Oak Ridge National Laboratory
P.O. Box 2008, Oak Ridge, TN 37831-6115
Phone: (865) 574-5082, E-mail: maziaszpj@ornl.gov

Objective

The main objective of this program is to work with commercial materials suppliers (foil and thin sheet) and recuperator manufacturers to enable upgraded recuperators to be made from cost effective alloys with improved performance and temperature capability. The near term goal is better performance to or above 704^{o}C (1300^{o}F), and the longer-term goal is reliable performance at 760^{o}C (1400^{o}F) and higher.

Highlights

Materials for use to about 704^{o}C (1300^{o}F)
ORNL initiated a joint project with Allegheny-Ludlum Technical Center to modify commercial-scale processing to improve the creep-resistance of sheet and foils of standard 347 stainless steel at 700-750^{o}C. Preliminary data on 10 mil sheet indicates clear changes in grain size distribution and indicate at least a 15-20% improvement in creep resistance at 700-750^{o}C.

Materials for use at 760^{o}C (1400^{o}F) or higher
Commercial 3 mil foil of HR120 has been obtained by ORNL from Elgiloy Specialty Metals (Elgin, IL), and is being creep-tested at 704^{o}C/152 MPa and 750^{o}C/100 MPa. The test at 704^{o}C ruptured after about 900 h with good ductility, and the test at 750^{o}C continues.

Technical Progress

Recuperator Component Analysis

Several different microturbine OEMs have provided pieces of fresh and engine-tested PFR and PSR recuperators made from standard 347 stainless steel for analysis and testing and characterization continues this quarter. These components are manufactured from coils of standard, commercial 347 steel that range from 3-4 mil foil to up to 10 mil sheet, and include the additional manufacturing steps of welding and/or brazing. ORNL is characterizing the engine-tested components and measuring the changes relative to fresh (as-manufactured) components. Detailed component analysis will be reported to each OEM, and will be used to help define specific advanced material solutions tailored to achieving better performance and temperature capability for the various kinds of recuperators.

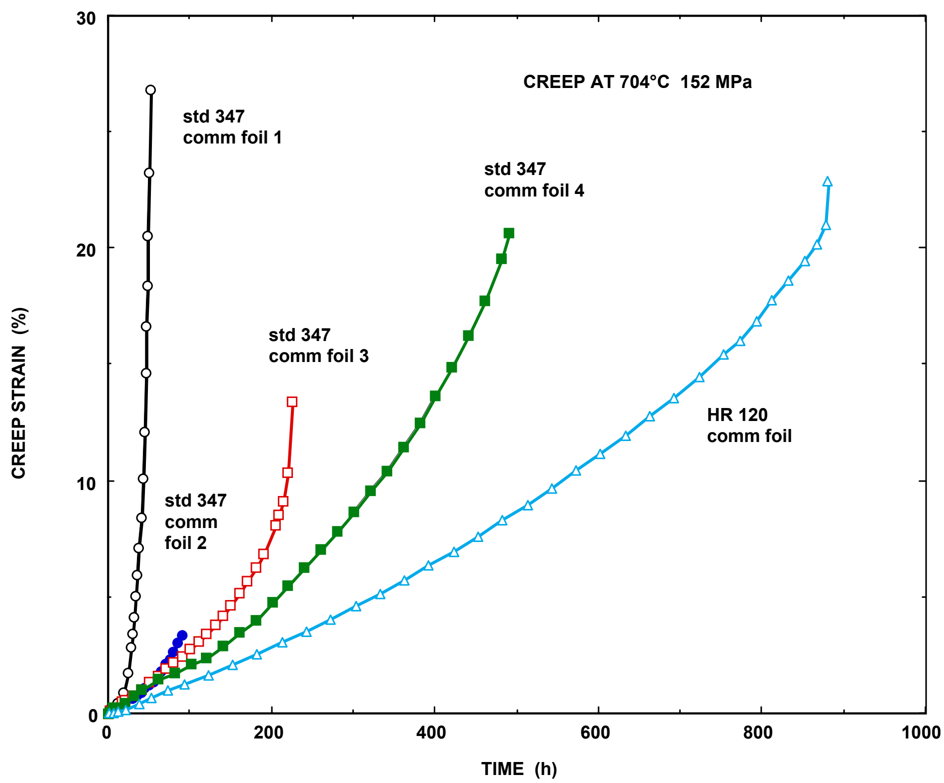

Figure 1 – ORNL creep testing of various standard commercial 347 stainless steel foils and sheet supplied by recuperator manufacturers. This shows the range of properties for standard products, and will be the baseline to define the improvements that can be achieved standard 347 with modified processing or in modified 347 stainless steels. Testing of commercial HR120 foil provided by Elgiloy is also included.

Selection and Commercial Scale-Up of Advanced Recuperator Materials:
a) Materials for use to about 704^{o}C (1300^{o}F)

To establish the performance baseline behavior for current recuperators made from standard 347 stainless steel, several different sheets and foils from several different commercial materials suppliers were provided by recuperator makers to ORNL for creep testing. Creep testing was done at 704^{o}C (1300^{o}F) and 152 MPa, and gave rupture lives ranging from 50 to 500 h, as shown in Fig. 1. Creep testing at 750^{o}C and 100 MPa gave rupture lives from 50 to 250 h for the same 347 sheets and foils.

ORNL initiated a joint project with Allegheny-Ludlum Technical Center to modify processing to improve the creep-resistance of sheet and foils of standard 347 stainless steel at 700-750^{o}C. The objective is to provide commercial materials that Ingersoll Rand

and Capstone can use to produce recuperator components with improved creep-resistance at about 700°C or slightly above, relative to currently available steel. Trial runs of 10 mil 347 steel sheet are being creep tested at 704°C/152 MPa and 750°C/100 MPa, and checked for microstructure. Preliminary data indicates clear changes in grain size distribution and indicate at least a 15-20% improvement in creep resistance. These data will determine the processing parameters for a commercial processing run to produce the 10 mil sheet required by Ingersoll Rand next quarter, and to produce intermediate material for further processing into various 3-5 mil thick foils with similar modifications to boost creep resistance. These processing parameters can also be used to produce sheet and foils from developmental commercial-sized heats of the new ORNL modified 347 stainless steels.

Oxidation testing of ORNL modified 347 steels continued at 650-800°C this quarter, and microstructural analysis of specimens tested at 800°C clearly indicates that these modified 347 steels are much more resistant to the formation of iron-rich oxide nodules that trigger severe break-away oxidation in water vapor.

b) Materials for use at 760°C (1400°F) or higher

HR 120 (Fe-25Cr-35Ni) is one of the more promising commercially available material with significantly better creep-resistance and corrosion-resistance in this temperature range at 3-4 times the cost of 347 stainless steel. Commercial 3 mil foil of HR120 has been obtained by ORNL from Elgiloy Specialty Metals (Elgin, IL), and is being creep-tested at 704°C/152 MPa and 750°C/100 MPa. The test at 704°C rupture after about 900 h with good ductility, and the test at 750°C continues.

Status of Milestones

FY2003 – Produce standard 347 steel with modified commercial processing to maximize creep resistance for sheet and foil gages. Certify properties and provide sufficient creep-resistant 347 steel to microturbine OEMs to manufacture recuperators with improved performance for use at or slightly above 700°C (April 2003). On schedule.

Industry Interactions

Microturbine OEM Ingersoll-Rand Energy Systems has agreed to take standard 347 sheet and foils being processed by Allegheny-Ludlum and ORNL for improved creep resistance, and has supplied the specific details on sizes and widths require for recuperator manufacturing. Discussions with Capstone to define their interest in obtaining foils of standard 347 for recuperator manufacturing continue.

Problems Encountered

None

Publications/Presentations

P. J. Maziasz and R. W. Swindewan, “Overview of Selection, Performance, and Development of Austenitic Stainless Steels for High-Temperature Applications,” was an invited talk presented at the Plenary Session of the ASM Stainless Steels and Specialty Materials Conference, held October 7-9, 2002 in Columbus, OH

P. J. Maziasz, B. A. Pint, R. W. Swindeman, K L. More and E. Lara-Curzio, “Advanced Stainless Steels and Alloys for High Temperature Recuperators,” presented at the ASM Distributed Energy Resources Conference, held October 7-9, 2002 in Columbus, OH.

Invention Disclosure on Engineered Microstructures for Improved Heat Resistance of Stainless Steels and Alloys for Thin-Section/Foil Applications filed with ORNL on September 22, 2002.

Recuperator Alloys – Composition Optimization for Corrosion Resistance

B. A. Pint and R. Peraldi
Metals and Ceramics Division
Oak Ridge National Laboratory
Oak Ridge, TN 37831-6156
Phone: (865) 576-2897, E-mail: pintba@ornl.gov

Objective

In order to provide a clear, fundamental understanding of alloy composition effects on corrosion resistance of stainless steel components used in recuperators, the oxidation behavior of model alloys is being studied. The first phase of this study narrowed the range of Cr and Ni contents required to minimize the accelerated corrosion attack caused by water vapor at 650°-800°C. Other factors that continue to be investigated include the effects of temperature, alloy grain size, phase composition and minor alloy additions. These composition and microstructure effects also will provide data for life-prediction models and may suggest a mechanistic explanation for the effect of water vapor on the oxidation of steels. This information will be used to select cost-effective alloys for higher temperature recuperators.

Highlights

Grain size has been shown to be an important factor for the corrosion resistance of both austenitic (type 347 stainless steel) and ferritic (Fe-16%Cr) alloys in air with 10%H_2O. In both cases, a finer grain size showed reduced susceptibility for the accelerated attack caused by water vapor. Initial results are shown for the second series of model alloys with 16-20%Cr, 15-20%Ni and various additions of Mn, Si and La. The alloys with 20%Cr and Mn and Si additions show the best overall performance in humid air from 650°C-800°C.

Technical Progress

<u>Experimental Procedure</u>

As outlined in previous reports, model alloys were vacuum induction melted and cast in a water-chilled copper mold. The chemical composition of the cast alloys was examined using inductively coupled plasma analysis and those results are reported in mass%, Table I. Pieces of cast material were then hot forged and hot rolled at 1100°C to 2.5mm thickness, followed by cold rolling to 1.25mm. The sheets were then annealed under Ar + 4%H_2, the ferritics for 2min at 900°C and the austenitics for 2 min at 1000°C. Average grain sizes are listed in Table I. Foil (≈100µm) specimens made commercially (supplied by Allegheny-Ludlum) or at ORNL also were examined. Oxidation specimens (≈1 or 0.1x12x18mm) were cut from the rolled plate materials and were polished to 600-grit SiC paper and cleaned in acetone and methanol prior to oxidation. The specimens were oxidized in dry air or air + 10vol.% water vapor with 100h cycles at 650°, 700° and 800°C.

<u>Oxidation Results</u>

Figure 1 shows results for fine- and coarse-grained type 347 foil during 100h cycles at 650°-800°C. At each temperature, the fine-grained (mill-rolled, ≈10µm) foil showed a delayed onset of accelerated

Table I. Alloy chemical compositions (weight %) and average grain sizes (μm).

	Cr	Ni	Mn	Si	Other	Grain Size
Type 347	17	11	1.6	0.6	0.6Nb	40μm
Fe 16Cr 15Ni	15.8	14.8	<	<		n.d.
Fe-16Cr-20Ni	15.7	19.5	<	<		19μm
Fe-20Cr-15Ni	19.9	15.3	<	<		n.d.
Fe-20Cr-20Ni	19.7	20.1	<	0.01		14
Fe-20Cr-30Ni	19.6	30.1	<	0.01		13
Fe-16/15+MS	15.9	14.9	1.74	0.24		~15
Fe-16/20+MS	15.8	19.7	1.72	0.24		~15
Fe-20/15+MS	19.8	14.9	1.70	0.24		~15
Fe-20/20+MS	19.8	19.8	1.69	0.25	0.01Ce	~15
Fe-20/20+Etc	20.9	20.8	>2	0.24	Nb	n.d.
Fe-12Cr	12.6	<	<	<		81μm
Fe-16Cr	15.7	<	<	<		97
Fe-20Cr	19.6	<	<	<		84
Fe-16Cr+Si	16.1	<	<	0.17		100
Fe-16Cr-1Mn	16.0	0.01	1.1	0.01<		88
Fe-16Cr+TiB_2	16.1	<	<	<	0.3Ti, 0.1B	~20

< indicates below the detectability limit of <0.01%

attack compared to the coarse-grained (ORNL-rolled, ≈40μm) material which almost immediately showed accelerated attack at each temperature. At 700°C, the fine-grained foil has not shown accelerated attack after 3800h of testing. This difference may be related to the different surface finish

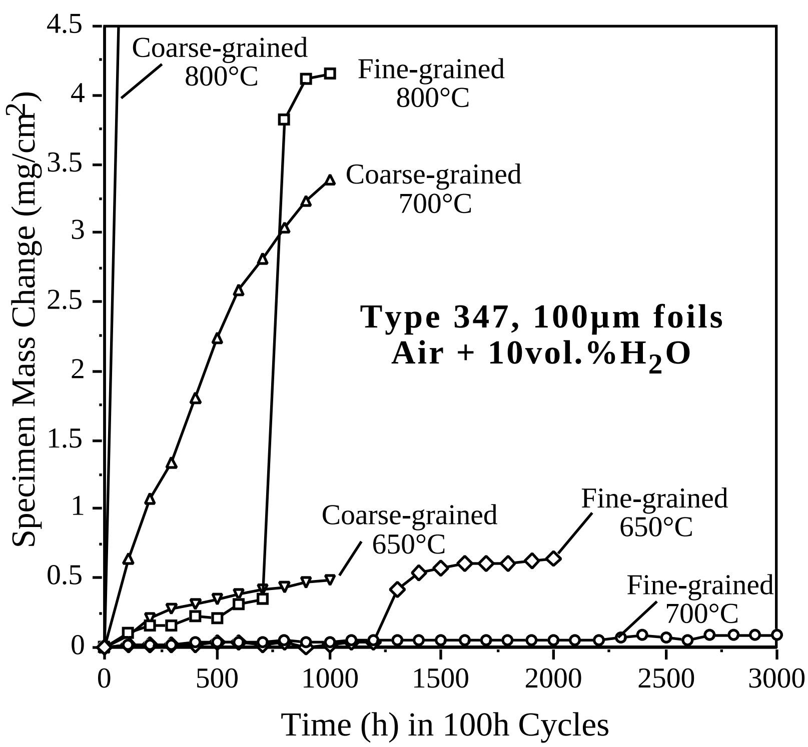

Figure 1. Mass change of stainless steel foils during 100h cycles at 700° and 800° in dry air or air plus 10% water vapor.

obtained in the two processes. However, the faster scale growth at 800°C would be less likely to be strongly affected by surface finish than grain size, which affects the flux of Cr in the alloy diffusing to the oxidation front. Avoiding surface Cr depletion in the fine-grained foil is likely a strong factor in delaying the onset of accelerated attack.

Figure 2 compares the mass changes of ferritic sheet specimens after 5, 100h cycles at 700°C in dry air to air with 10%H_2O. In dry air, the majority of alloys exhibit mass gains of 0.1-0.3mg/cm^2. Exceptions are for Fe-10%Cr and for Fe-16%Cr-0.1Ti. The low Cr content of the former alloy is not sufficient to form a protective scale under these conditions. As has been shown in a previous report, in humid air, most of the alloys showed higher mass gains which is typical of the accelerated attack caused by the addition of water vapor. The exception is the alloy containing a TiB_2 addition, which was the only addition which resulted in a finer grain size, Table I and Figures 3a and 3b. The TiB_2-dispersed Fe-16%Cr specimen showed better performance than even a Fe-20%Cr specimen, indicating the importance of a finer grain size for reducing the detrimental role of water vapor.

Based on the results from the first series of austenitic model alloys and the ferritic model alloys with various minor additions, a new series of model austenitic alloys were fabricated using the same processing steps. This series focused on Cr contents of 16-20% and Ni contents of 15-20% and minor alloy additions of Mn, Si and La, which have shown the most promising benefits. In this case, these minor additions do not change the alloy grain size. For example, the similar grain sizes of Fe-20Cr-20Ni with and without Mn and Si additions are shown in Figures 3c and 3d. Initial oxidation results for this series of alloys in humid air at 650°, 700° and 800°C are shown in Figure 4. These mass change results are complicated because of the competition between mass gains due to the formation of thick Fe-rich scales and the spallation of these thick scales. Protective behavior is noted by

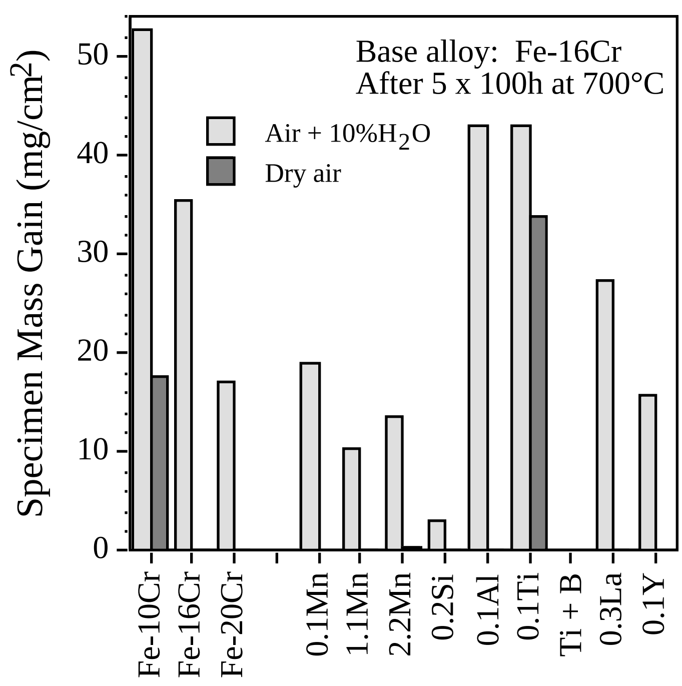

Figure 2. Specimen mass gain after 5, 100h cycles at 700°C in dry air and air + 10vol.%H_2O for various Fe-Cr alloys. The mass gains in humid air were much higher than those in dry air.

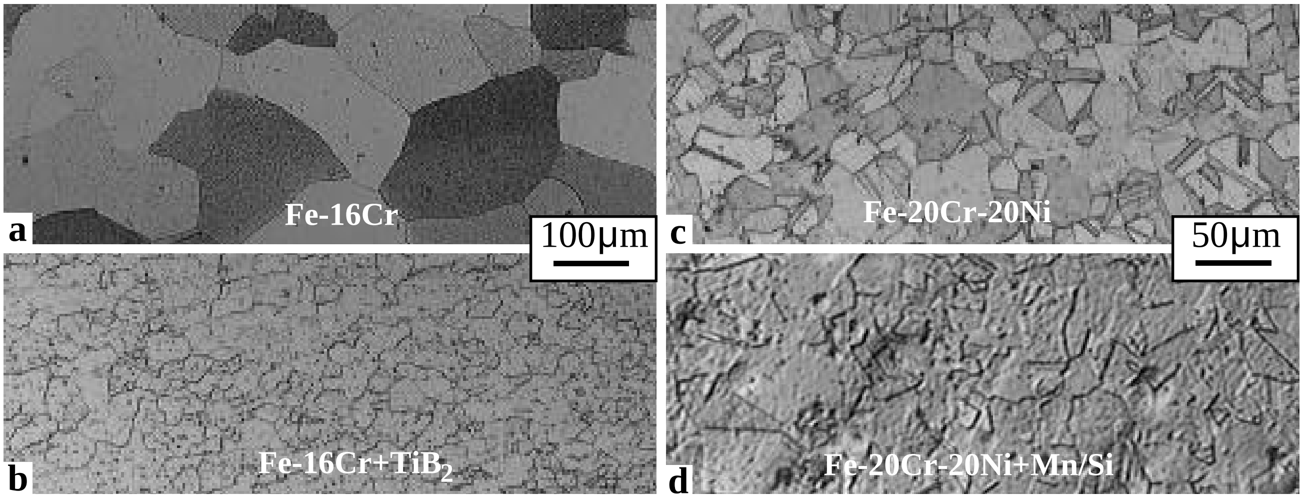

Figure 3. Light microscopy of rolled model alloys (a) Fe-16Cr (b) Fe-16Cr + TiB_2, (c) Fe-20Cr-20Ni and (d) Fe-20Cr-20Ni+Mn/Si.

minimal mass change with the formation of a thin protective scale. From the previous series of austenitic alloys, the resistance to accelerated attack improved with increasing Cr and Ni contents and some benefit was associated with reducing the grain size from as-cast (coarse-grained) specimens to rolled (fine-grained) specimens. However, even better performance was noted with additions of Mn and Si, Table I. The addition of Mn and Si did not result in protective behavior for the Fe-16Cr-15Ni but the other compositions formed a protective oxide scale for up to 1000h at each temperature. Long-term testing will continue for the most promising alloys along with characterization of the reaction products.

Status of Milestones

Draft a report summarizing results on the use of minor alloy additions to improve corrosion performance in exhaust gas environments. (January 2003)

Industry Interactions

Discussed the oxidation performance of 321 and 347 stainless steels with Alvin Nakagawa from Northrop Grumman Marine Systems in October 2002.

Discussed the use of Haynes 214, PM2000 and alloy 625 in a high temperature recuperator with Joe Daly from Fuel Cell Energy in December 2002.

Problems Encountered

None.

Publications/Presentations

None

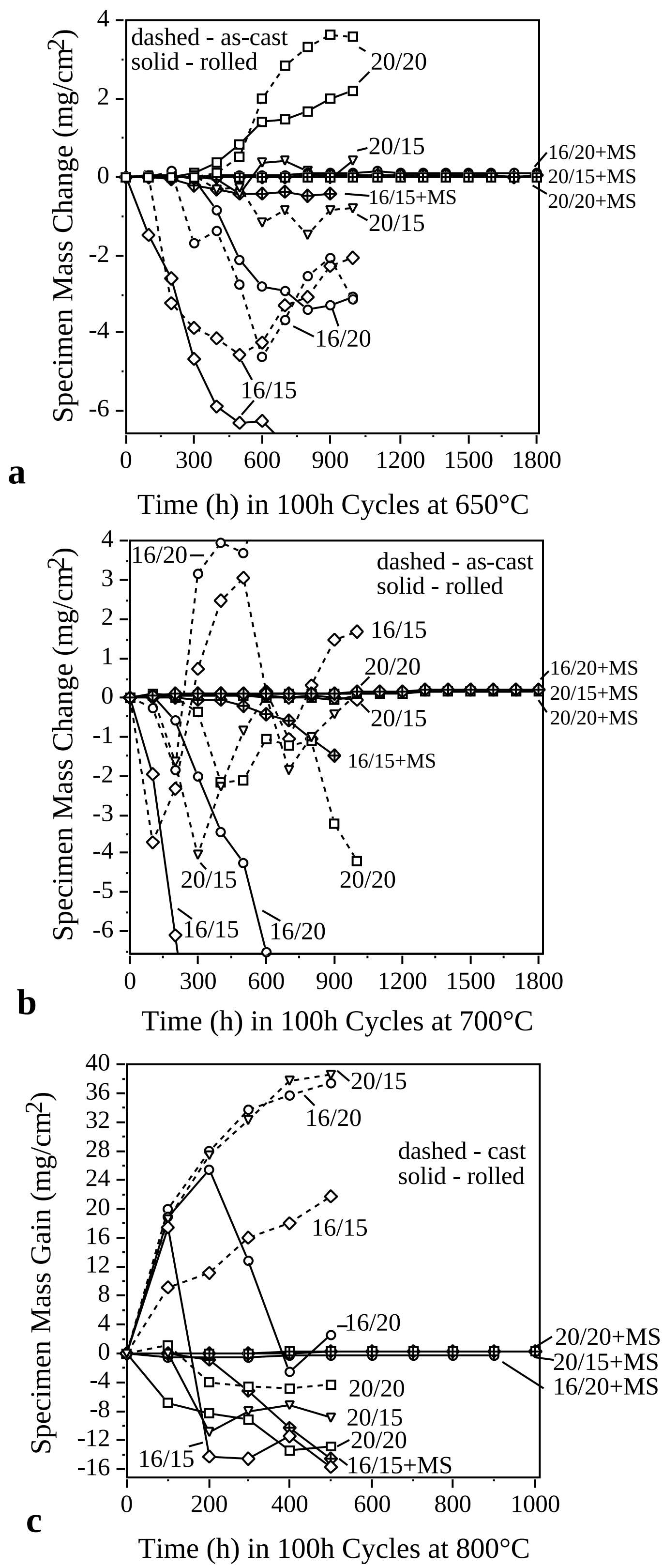

Figure 4. Specimen mass changes for as-cast (dashed lines) and rolled (solid lines) model Fe-Cr-Ni alloys (specified by their Cr/Ni contents) some of which contain Mn and Si (MS) during 100h cycles in air plus 10%H_2O at (a) 650°C, (b) 700°C and (c) 800°C.

Recuperator Materials Testing and Evaluation

Edgar Lara-Curzio
Metals and Ceramics Division
Oak Ridge National Laboratory
P.O. Box 2008, Oak Ridge, TN 37831-6069
Phone: (865) 574-1749, E-mail: laracurzioe@ornl.gov

Objective

The objective of this sub-task is to screen and evaluate candidate materials for the next generation of advanced microturbine recuperators. To attain this objective, a commercially-available microturbine was acquired and in coordination and collaboration with its manufacturer, it was modified to operate at recuperator inlet temperatures as high as 843°C. The durability of candidate recuperator materials will be determined by placing test specimens at a location upstream of the recuperator, followed by determination of the evolution of the material's physical and mechanical properties as a function of time of exposure. During exposure tests inside the microturbine, it will be possible to subject test specimens to various levels of mechanical stress by using a specially-designed sample holder and pressurized air. The selection of materials to be evaluated in the modified microturbine will be made in coordination and collaboration with other tasks of this program and with manufacturers of microturbines and recuperators.

Highlights

- ORNL's microturbine testing facility was successfully repaired after the pre-charge circuit in the load control module failed for the second time since the microturbine was commissioned in 2001. The pre-charge circuit contains resistors that are used to limit surge currents into the DC Bus upon power up. As part of the repairs, the electromagnetic interference (EMI) board also had to be replaced.

- Edgar Lara-Curzio became a Capstone Authorized Service Provider.

Technical progress

An important objective of this task is to evaluate the evolution of mechanical and physical properties of microturbine recuperator materials as a function of service history. To accomplish this objective, microturbine recuperators that have been decommissioned after field operation are being evaluated to characterize their microstructure and to determine their residual mechanical and physical properties. During the reporting period, an agreement was established with CANMET of Canada to receive two additional Honeywell 75 kW Parallon microturbines and two 30kW Capstone recuperators.

During the reporting period work continued on the evaluation of a Solar Recuperator that had been retrieved from a Honeywell 75 kW Parallon microturbine that had been installed at the University of Maryland on June, 2000, and decommissioned on October 2001. On July 2001, both the recuperator and engine core were replaced, and the second recuperator was exposed for a total of approximately 500 hours in 8-hour daily cycles between 9:00 AM and 5:00 PM. The microturbine was operated at a demand of 75 kW and speed of 65,000 RPM. The exhaust temperature was 260°C, but the actual TET is unknown.

Figure 1 shows a photograph of the 347 stainless steel recuperator after it had been removed from its housing. The inlet and outlet manifolds are clearly visible in the photograph. The recuperator was sectioned into smaller parts using a torch, and each one of those sections was then sub-sectioned by electric discharge machining to obtain strips 9 inches long and 0.5 inches wide.

Figure 1. Photograph of Solar recuperator retrieved from 75kW Parallon microturbine. The inlet and outlet manifolds for compressed air are clearly visible in the picture.

Figure 2 is a schematic representation of the recuperator indicating the locations from where sections were removed, which were subsequently sectioned into strips. Figure 3 shows a photograph of one of these strips while Figure 4 is a photograph of the cross-sectional area of one of the strips that was used for tensile evaluation.

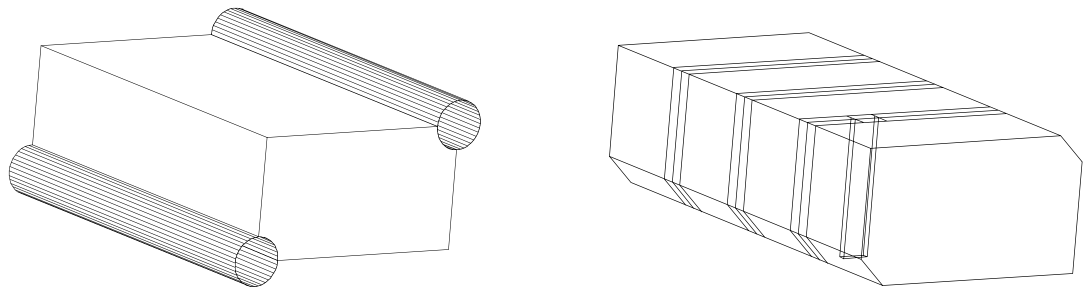

(a) (b)

Figure 2. Schematics showing (a) recuperator with manifolds; (b) locations from which strips were removed for tensile evaluation.

Although the cross-sectional area of the strips is not uniform along their length, they were evaluated under tensile loading to compare the effect of location on the mechanical properties of the material.

Tensile tests were carried out using a servohydraulic testing machine equipped with hydraulic grips and with a one-inch gauge length clip-on extensometer. Figure 5 shows a typical stress versus strain curve obtained from the tensile evaluation of one of the recuperator strips. Also shown are the lines that were used to determine the values of the 0.02% and 0.2 yield strength. The tensile stress-strain curves exhibit a linear region, followed by non-linear behavior. The increase of stress with strain towards the end of the test is associated with the unfolding of the foil corrugations and is not intrinsic to the behavior of the material.

Figure 3. Photograph of recuperator strip used to evaluate tensile stress-strain behavior. Total length of strip is 9 inches.

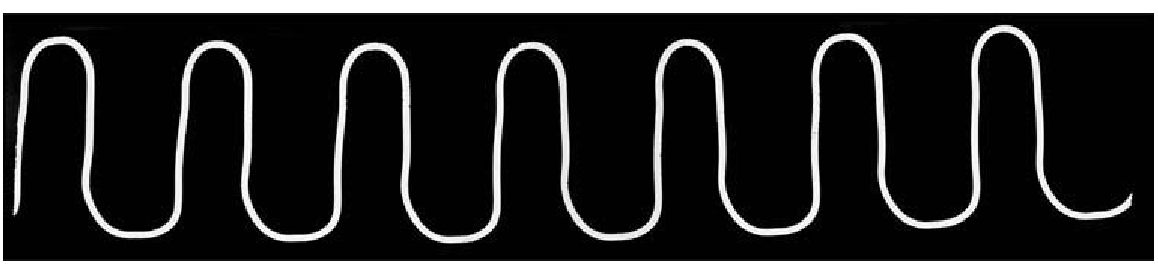

Figure 4. Cross-sectional image of recuperator cell used for tensile testing. The peak to valley distance is 0.089 inches.

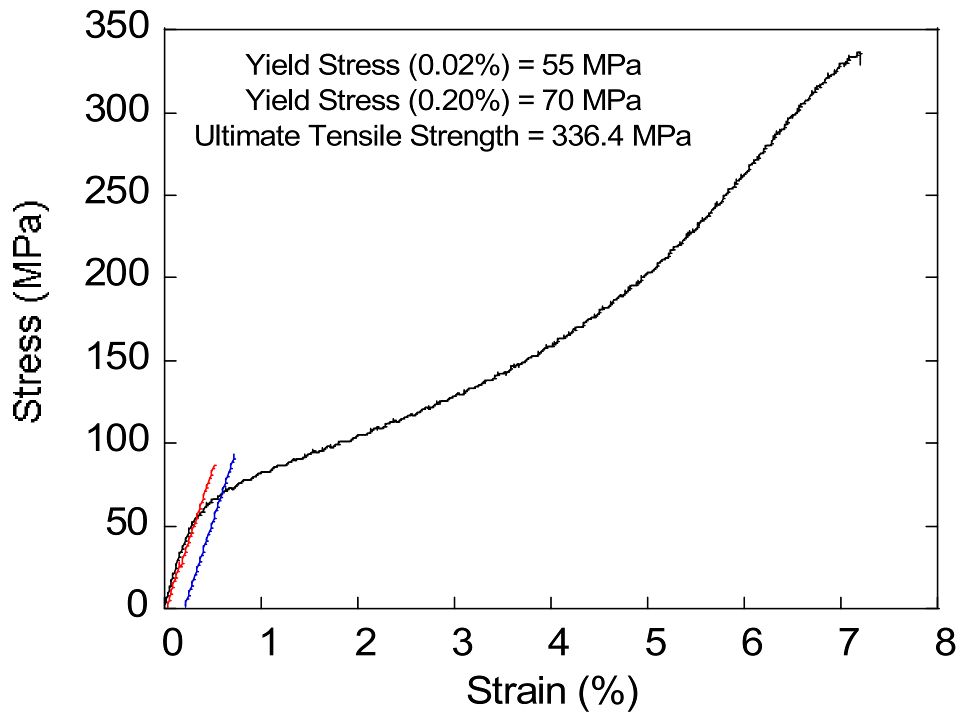

Figure 5. Typical stress-strain curve obtained from tensile evaluation of corrugated recuperator foils.

It was found that the tensile behavior of the corrugated foils was reproducible in a given section of the recuperator as illustrated in Figure 6, which shows a collection of 14 stress-strain curves obtained from the evaluation of strips from the same section of the recuperator.

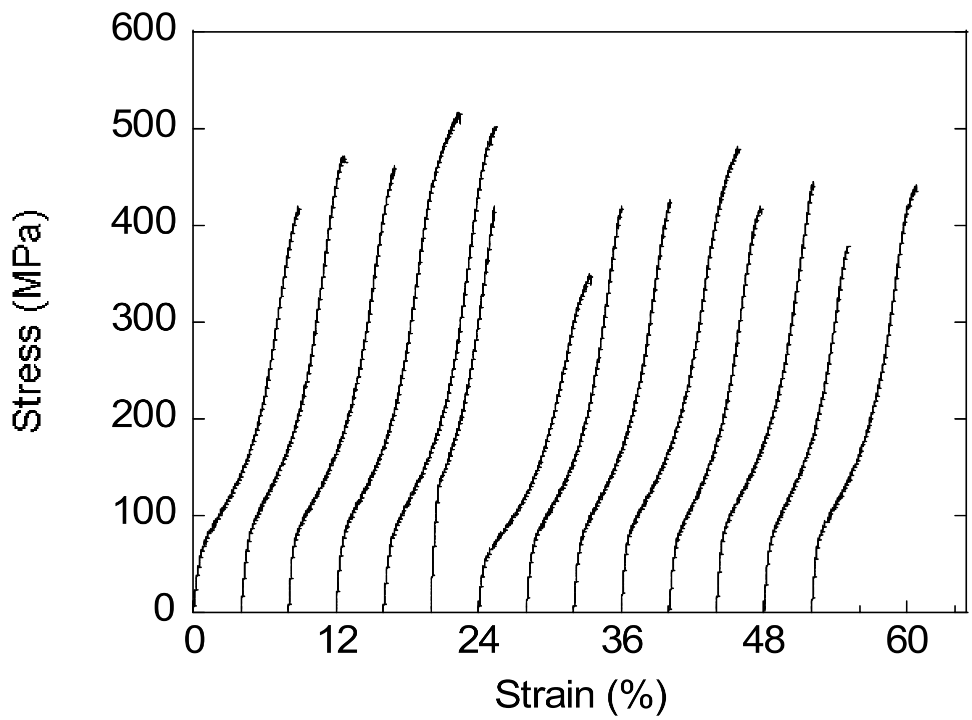

Figure 6. Collection of stress-strain curves for section 6-5 of the recuperator.

Figures 7, 8 and 9 summarize the results for the 0.02% yield strength, 0.2% yield strength and the ultimate tensile strength, respectively as a function of location in the recuperator. The error bars correspond to one standard deviation with respect to the mean value. An analysis of variance of these results indicated that at the 95% level of confidence, the mean values were not equivalent, i.e. - the magnitude of the strength values does depend on the location of the recuperator.

Ongoing work is focused on the microstructural characterization of these materials in order to understand the trends of these results.

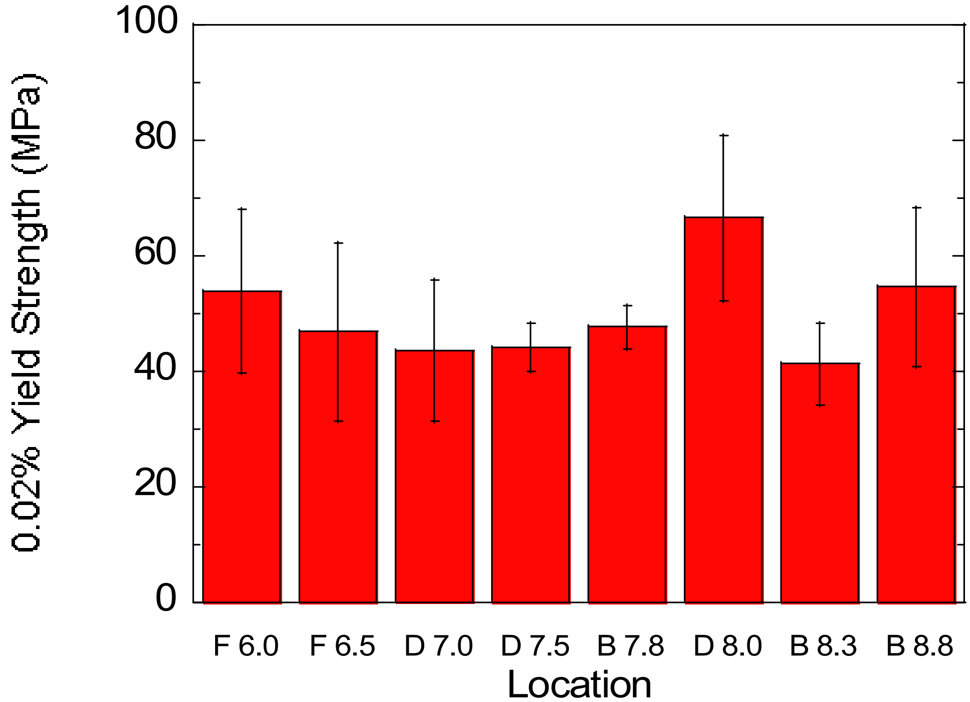

Figure 7. 0.02% yield strength of foils as a function of location.

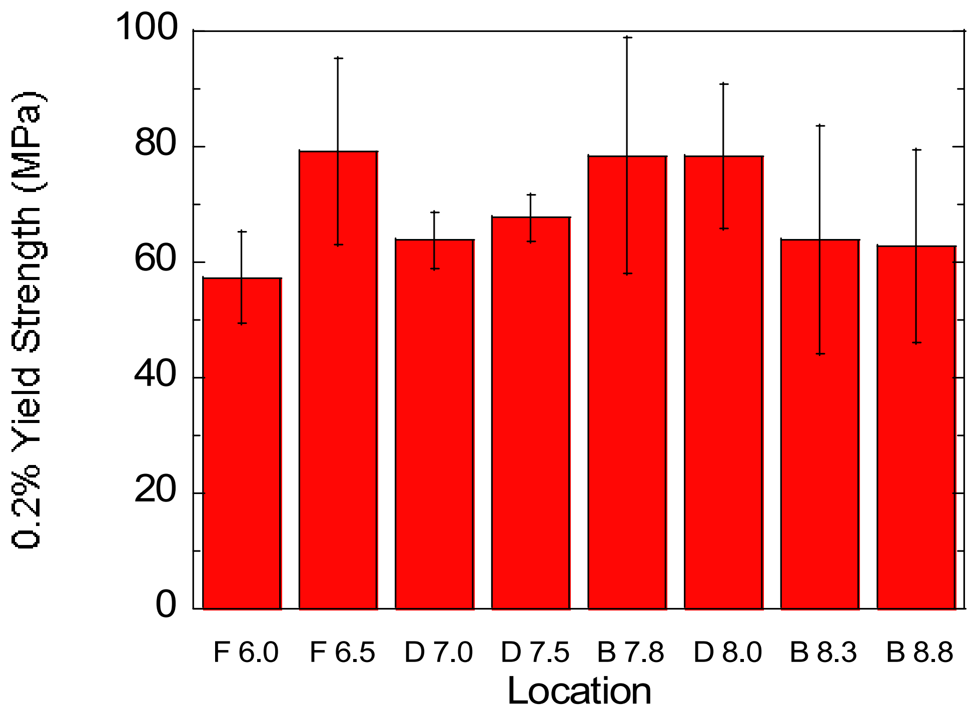

Figure 8. 0.2% yield strength of foils as a function of location.

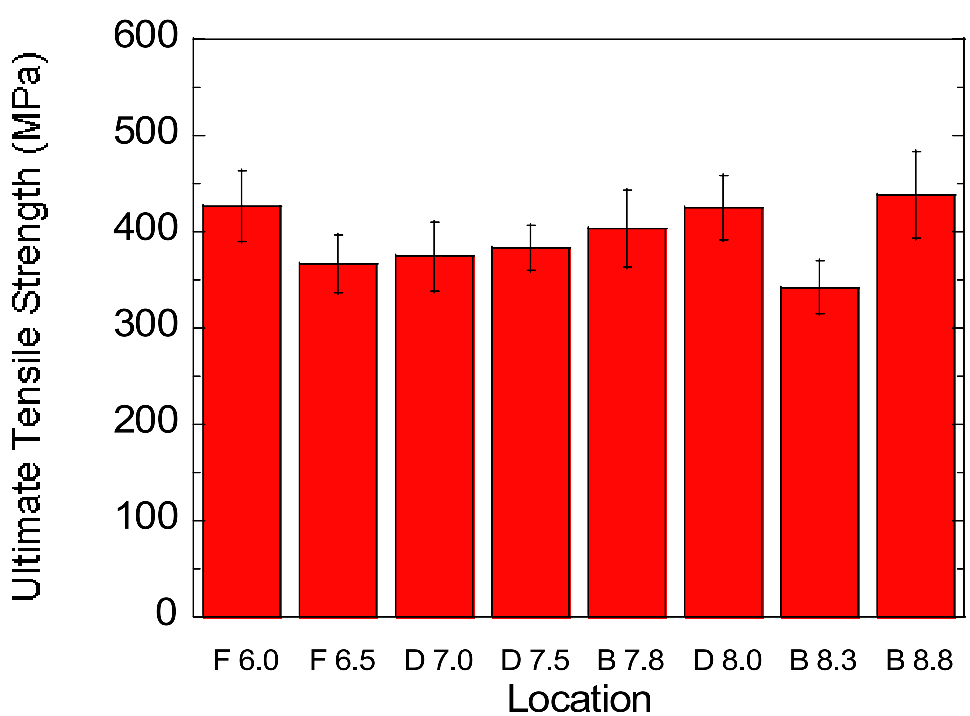

Figure 9. Ultimate tensile strength of foils as a function of location.

Status of Milestones

On schedule

Industry Interactions

Edgar Lara-Curzio became a Capstone Authorized Service Provider after attending a one-week long training course at Capstone Turbine Inc., Chatsworth, CA 92918.

Problems encountered

ORNL's microturbine testing facility was successfully repaired after the pre-charge circuit in the load control module of the power electronics package failed for the second time since the microturbine was commissioned in 2001. The pre-charge circuit contains resistors that are used to limit surge currents into the DC bus upon power up. As part of the repairs, the electromagnetic interference (EMI) board also had to be replaced. Figure 10 shows the photograph of the damage in the EMI board.

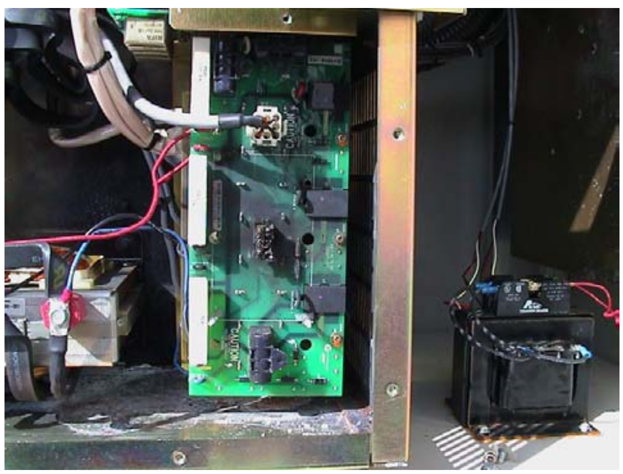

Figure 10. Photograph showing damaged EMI filter board in power electronics module of ORNL's microturbine.

Publications/Presentations

None

Reference or Trips/Meetings

None